Protoplasma (1992) 166: 8–20

PROTOPLASMA

Microtubules of the flagellar apparatus are active during prey capture in the chrysophycean alga *Epipyxis pulchra*

R. A. Andersen[1,*] and **R. Wetherbee**[2]

[1] Bigelow Laboratory for Ocean Sciences, West Boothbay Harbor, Maine, and [2] School of Botany, University of Melbourne, Melbourne, Victoria

Received June 21, 1991
Accepted June 21, 1991

Summary. The flagellar apparatus of *Epipyxis pulchra* (Chrysophyceae) and its role in phagotrophy is described. Prior to feeding, the cell elongates forming a basal stalk, and the flagellar apparatus moves away from the contractile vacuole/nucleus complex. In feeding cells the flagellar apparatus consists of a striated rhizoplast, cytoplasmic microtubules nucleated from the short flagellum basal body, three microtubular roots (R_1, R_3 with tubules *a–f*, R_4) and cytoplasmic microtubules nucleated from R_1 and R_3 roots. The microtubules of the R_3 root split forming a small and a large loop under the short flagellum; the *a* microtubule forms the inner, smaller loop and the *f* microtubule forms the outer loop. After looping under the short flagellum, the *a* and *f* microtubules join and extend deep into the cell along a complex layered structure involving microtubules, the rhizoplast and a mitochondrion. When a food particle is captured between the flagella, the cell forms a feeding cup to engulf the particle. The rim of the developing cup forms as the distal end of the *f* microtubule slides up the complex layered structure, increasing the size of its loop under the short flagellum. Vesicles fuse between the loops of the *a* and *f* microtubules, increasing the surface area and depth of the cup. When the cup is fully formed, the food particle is moved into the cup. The *f* tubule returns to its normal position, closing the cup and forming a food vacuole.

Keywords: Cytoskeleton; Flagellar apparatus; Microtubular roots; Morphogenesis; Phagocytosis.

Introduction

Phagotrophy in chrysophyte algae has been known for over one hundred years. Early light microscopy studies describe flagellar motion drawing food particles to the cell surface where a large bubble-like vacuole forms to capture the prey (James-Clark 1867, Cienkowsky 1870, Saville-Kent 1880, Stokes 1885). Pascher (1910) observed that *Epipyxis* (= *Hyalobryon*) was not strictly autotrophic but feed on bacteria and small blue-green algae. Phagotrophic chrysophytes play an important role in microbial food webs, often recycling or mineralizing carbon, phosphorous, nitrogen and other ecologically important elements (see Sanders and Porter 1988). However, despite the long record of its occurrence and the recognition of the important ecological role it plays, the cellular mechanism for chrysophyte phagotrophy has not been described.

The chrysophycean alga *Epipyxis pulchra* supplements its energy derived from photosynthesis by phagocytizing bacteria. The flagella of *Epipyxis* capture and select prey, a process described using image enhanced video microscopy (Wetherbee and Andersen 1992). To summarize that process briefly, the flagellar beat creates water currents that draw food particles to the cell where they are captured and held between the flagella. A feeding cup forms quickly, the flagella "toss" the food particle into the cup, and the cup closes to engulf the food particle. The feeding cup forms near the base of the flagella. This led us to hypothesize a possible role of the flagellar roots in the formation and closure of the feeding cup. We investigated the ultrastructure of feeding cells, and in this paper we show that the feeding cup forms as the result of a precise movement of a specific flagellar root microtubule as it interacts with microtubular and fibrillar roots of the basal apparatus.

Materials and methods

Epipyxis pulchra Asmund et Hilliard was collected, isolated and brought into culture (Provasoli-Guillard Center for Culture of Ma-

* Correspondence and reprints: Bigelow Laboratory for Ocean Sciences, West Boothbay Harbor, ME 04575, U.S.A.

rine Phytoplankton, clone CCMP-382). Cells were grown in DYIII medium (Lehman 1976) enriched with soil water extract at approximately 15–20 °C with a 14 : 10 h light : dark cycle using an illumination of about 50 μE/cm² of cool white fluorescent light. Cells were fixed using several protocols: (1) Cells were collected from the air-water interface using a glass rod, rinsed into a fixative cocktail consisting of 2% glutaraldehyde and 1% osmium tetroxide in 0.05 M cacodylate buffer (pH 7), rinsed in distilled water, prestained in 0.05% uranyl acetate overnight, dehydrated through an ethanol series and two changes of propylene oxide, and embedded in Spurr's resin (Figs. 3 a and b, 4 d, 5 a–k, 7 c, and 11 a–d); (2) cells were placed on a microscope slide and observed, when most cells were extended and feeding, 0.5% osmium tetroxide in 0.1 M cacodylate buffer was squirted by pipette onto the cells. The cells were quickly rinsed from the slide using 2% glutaraldehyde and fixed for 25 min. Fixed cells were rinsed with buffer, dehydrated in a graded series of ethanol followed by two changes of propylene oxide, and embedded in Spurr's resin. Cells were stained overnight with uranyl acetate (1%) at the 70% ethanol dehydration step (Figs. 3 c, e, and f, and 4 a–c, e, and f); (3) cells were fixed as in (2) but without glutaraldehyde (Fig. 9 a–h).

Cytoskeletons were isolated by mixing cold cells (on crushed ice) with cold 0.1% Triton 100 in MT buffer (30 mM HEPES, 5 mM $MgSO_4 \cdot 7H_2O$, 25 mM KCl, 5 mM EGTA at pH 7) for 5 min. The preparation was rinsed twice with cold MT buffer and the cytoskeletons were fixed with 2% paraformaldehyde. Whole cells were fixed with 0.25% osmium tetroxide, 2% glutaraldehyde or 2% paraformaldehyde. Cytoskeletons and cells were prepared for immunological study by rinsing with phosphate buffered saline (PBS), treating with sodium borohydrate for 30 min, and rinsing with PBS. They were placed on polylysine coated coverslips, incubated 1 h at 37 °C with the primary antibody, rinsed with PBS, incubated 1 h at 37 °C with the secondary antibody, and mounted onto microscope slides using Movial mounting medium. The primary antibodies were a monoclonal anti-tubulin (courtesy Dr. David Asai), a monoclonal anti-actin (Amersham Corp.), and a polyclonal anti-centrin (courtesy Dr. J. Salisbury). The secondary antibodies were a goat-anti-mouse antibody labeled with FITC and a sheep-anti-rabbit antibody labeled with Rhodamine. *Apedinella*, an organism known to react with all three primary antibodies (Koutoulis et al. 1988), was used as a control.

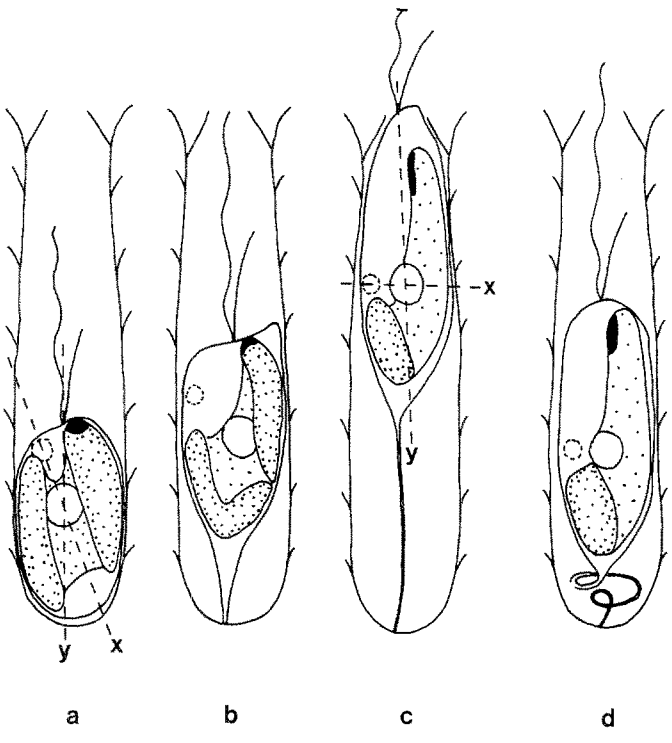

Fig. 1

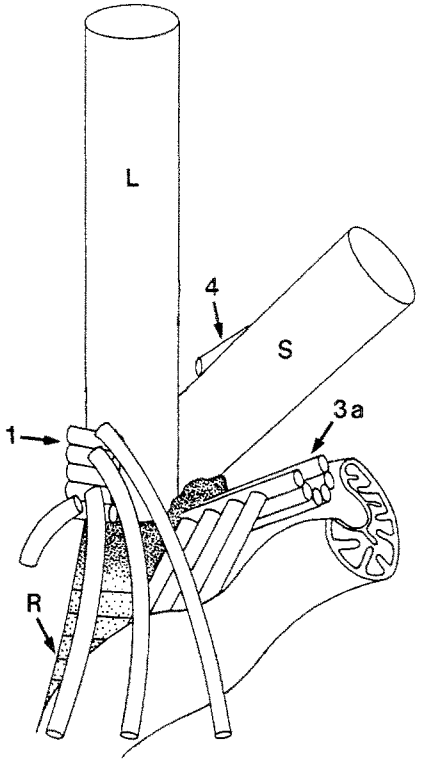

Fig. 2

Fig. 1. a A nonfeeding vegetative cell lacking a stalk. The x-axis passes through the contractile vacuole and nucleus while the y-axis passes through the flagellar basal bodies and nucleus. **b** A cell undergoing morphogenesis to the feeding state, showing stalk formation and early stages of flagellar apparatus relocation. **c** A feeding cell showing the fully formed stalk and relocated flagellar apparatus. The x- and y-axes are the same as described in **a. d** A feeding cell that contracted into the lorica by coiling its stalk; the flagellar apparatus and chloroplast do not change positions

Fig. 2. Diagrammatic illustration of the flagellar base region showing the microtubular roots and rhizoplast. The *a* tubule of the R_3 microtubular root is identified; tubules *b–f* lie sequentially adjacent to the *a* tubule. Cytoplasmic microtubules extend from the R_1 microtubular root and the R_3 cytoplasmic microtubules extend from the R_3 microtubular root. The long flagellum is directed anteriorly, the short flagellum is directed ventrally, and the right side is towards the reader

Results

Morphogenesis to the feeding state

The nonfeeding cell resides deep within the scaly lorica; its chloroplast is compactly spiral and the eyespot lies adjacent to the short flagellum (Fig. 1 a). The cell undergoes a substantial change in morphology as it converts to the feeding mode. The cell elongates, forming a short, broad stalk (Fig. 1 b). Within 5 to 10 min the cell is fully elongate, a long narrow stalk is present and the cell extends slightly beyond the lorica opening (Fig. 1 c). At irregular intervals during this change in shape morphogenesis, the cell jumps and contracts inside the lorica. Once the cell is fully extended, it retains the ability to contract. For example, if a cell is disturbed by bumping the microscope, it instantly contracts into the lorica, facilitated by the coiling of the stalk (Fig. 1 d). However, the cell does not return to the morphological state of the nonfeeding cell, and if the perturbation is temporary, the cell returns to the extended feeding state within about 30 s by straightening the stalk.

The most obvious change during the feeding state morphogenesis is the relative displacement of the flagella away from other organelles, especially the contractile vacuole, nucleus, chloroplast and eyespot. By drawing two axes, one through the flagellar bases and the nucleus and the other through the contractile vacuole and nucleus, the distribution of organelles in nonfeeding and feeding cells is readily apparent (Fig. 1 a and c). Another obvious difference between nonfeeding and feeding cells is the position of eyespot relative to the short flagellum.

The ultrastructural changes from the nonfeeding to the feeding state are not described here, but it is necessary to mention these differences because usually the stalks of the elongate feeding cells contract and coil during fixation. By determining the position of the flagella relative to the eyespot and contractile vacuole, feeding cells that contract during fixation are distinguishable from nonfeeding cells.

Flagellar apparatus in feeding cells

The basal root apparatus consists of a large fibrillar root (rhizoplast), three microtubular roots, and microtubules nucleated from the microtubular roots and from the short flagellum basal body. The flagellar apparatus has one absolute configuration and the cell surfaces are named according to convention (Fig. 2). The three microtubular roots are labeled R_1, R_3, R_4; the R_2 root that occurs in many flagellates is absent in *Epipyxis*. The shortest is the R_1 root, being only about 600 nm long (Fig. 3). It consists of five stacked microtubules (Fig. 3 c) that lie dorsal to the long flagellum basal body (Fig. 3 a, b, e, and f). Microtubular organizing centers (MTOCs) along the root nucleate cytoplasmic microtubules (Fig. 3 a–c and e–f) that splay out and extend to the posterior of the cell. Additional cytoplasmic microtubules are nucleated from the short flagellum basal body (Fig. 3 a and f).

The R_3 root originates on the right side of the basal bodies and has six microtubules (*a–f*) organized as a U-shaped trough at its proximal end (Fig. 3 d–f). Tubules *b* through *e* are short; the *b* tubule is approximately 500 nm in length, the *e* tubule approximately 1.5 μm, and tubules *c* and *d* are intermediate in length. Tubules *a* and *f* are much longer and play a dynamic role during feeding cup formation.

The *a* and *f* tubules loop anticlockwise around and under the short flagellum (Fig. 3 a, b, and f). After forming separate loops under the short flagellum, the *a* and *f* tubules come together, pass under the basal bodies and extend deep into the cell (Fig. 4 d) where they are components of a complex layering of organelles (see below). The *a* and *f* tubules are heavily coated throughout their length, sometimes having a striated periodicity of 20–25 nm (Figs. 4 d–f and 9 a).

The proximal end of the R_3 root contains a MTOC and nucleates several (9–11) microtubules, here termed R_3 cytoplasmic microtubules (R_3CM) (Fig. 4 c) that extend posteriorly along a mitochondrion (Fig. 4 c and d, also Figs. 4 b and 5 e, f, and h–j). The R_3CM are not interconnected in our preparations, and serial sections through several cells show that the arrangement is not precise or consistent, although the majority of the R_3CM are adjacent to the mitochondrion surface (Fig. 5 e and f).

The R_4 root is a single microtubule that originates on the surface of the short flagellum (Fig. 3 b). It curves clockwise around and under the short flagellum (Fig. 4 a) and terminates (Fig. 3 a). On the left side of the cell the R_4 root and the *a* and *f* tubules of the R_3 root are closely associated (Figs. 3 a, b, f, 4 a, and 5 b), and this is important for feeding cup formation (see below). On the right side, however, there is always a space between the *a* and *f* tubules (Figs. 3 a and b, 4 b and e, and 5 b).

At the level of the basal bodies, tubules *a* and *f* are ventral to the short flagellum (Fig. 5 c and d). Posterior to the basal bodies the *a* and *f* tubules are associated closely with the left surface of the rhizoplast (Fig. 5 e). As the *a* and *f* tubules extend toward the nucleus, the

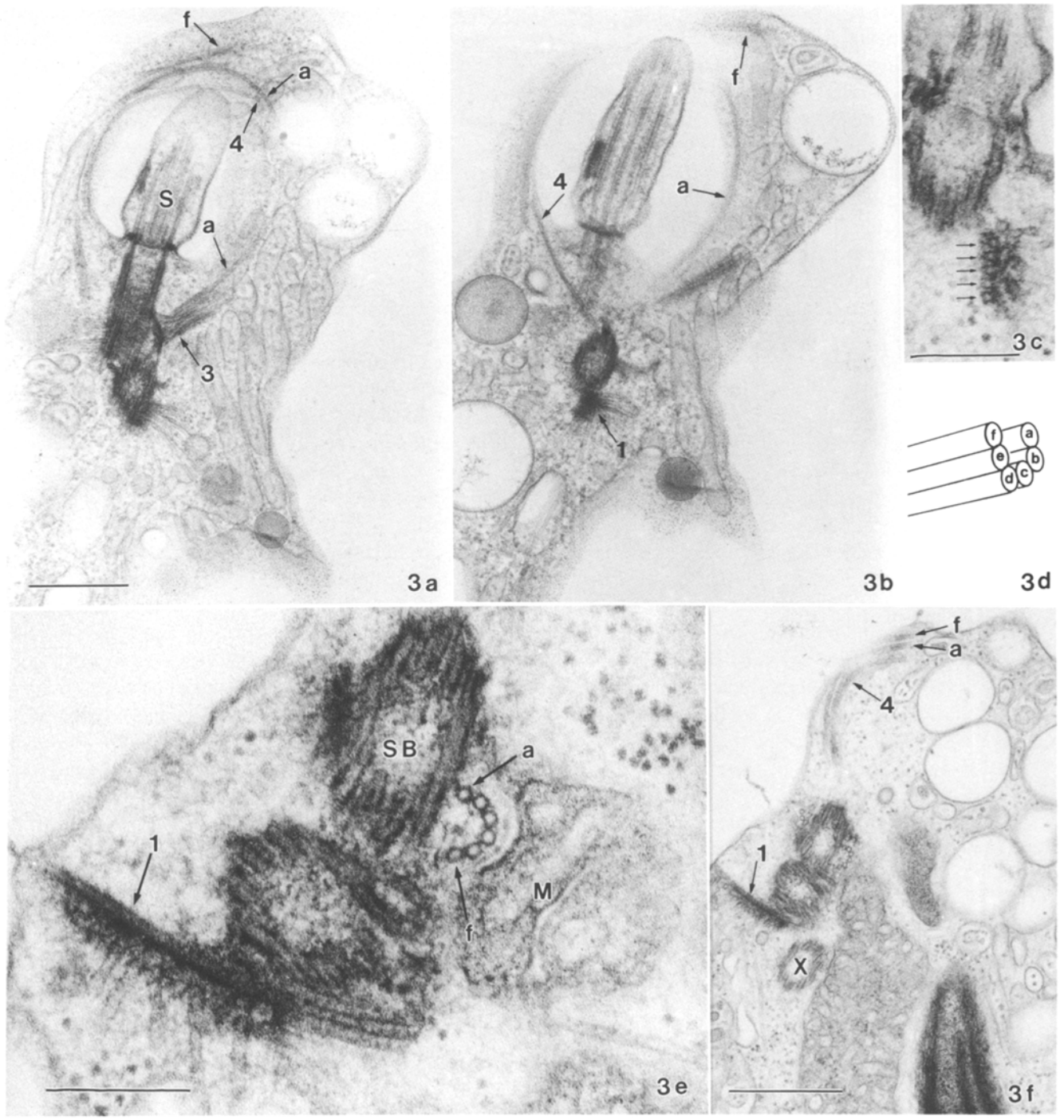

Abbreviations used in figures: a–f *a–f* microtubules of the R_3 root, respectively, B bacterium, E eyespot, L longitudinal flagellum, M mitochondrion, N nucleus, P plastid, R rhizoplast, S short flagellum, SB short flagellum basal body, X extra basal body, 1 R_1 microtubular root, 3 R_3 microtubular root, 3 a *a* tubule of the R_3 microtubular root, 4 R_4 microtubular root

Fig. 3. a and **b** Adjacent thick serial sections showing the R_1 microtubular root adjacent the long flagellum basal body, the origin of the R_3 microtubular root near the basal bodies and the R_4 microtubular root above the short flagellum basal body. The *a* and *f* tubules of the R_3 root form a loop around the short flagellum. The R_4 termination is indicated in **a. c** The five stacked microtubules that make up the R_1 root. 13° tilt. **d** A diagram illustrating the labelling for the microtubules of the R_3 root. **e** and **f** Adjacent thin serial sections showing the proximal end of the R_3 root. 10° tilt. **e** The six microtubules of the R_3 root form a semicircular profile in cross section, lying near the short flagellum basal body and the mitochondrion. The R_1 root is nucleating several cytoplasmic microtubules including one passing by the mitochondrion. **f** Microtubules *a* and *f* of the R_3 root and the single microtubule of the R_4 root lie on towards the ventral surface. Bar: 500 nm in a, b, and f; 200 nm in c and e

a tubule is closer to the dorsal surface of the cell while the *f* tubule lies closer to the ventral surface (Fig. 5 f). A large, straight and long rhizoplast extends posteriorly from the basal bodies (Fig. 4 c and d), and it is closely associated with the mitochondrion (Fig. 5 e and f). The distal ends of the *a* and *f* microtubules of the R_3 root lie along the left surface of the rhizoplast (Figs. 4 d and 5 e and f). The R_3CM lie between the rhizoplast and the mitochondrion (Figs. 4 c and 5 f and g). The complex layered structure consisting of the *a* and *f* tubules, the rhizoplast, the R_3CM and the mitochondrion, is illustrated in Fig. 6; it passes next to the eyespot in feeding cells (Fig. 4 c and d).

The *a* and *f* tubules of the R_3 root do not terminate at the same place, even in potentially feeding cells that are not actively forming feeding cups. The distal end of the *f* tubule is approximately 1 μm anterior to the distal end of the *a* tubule (Fig. 5 g–i). The *a* tubule terminates very near the nucleus (Fig. 5 j).

Using a primary antibody active against α-tubulin, flagellar and cytoplasmic microtubules are evident in whole cells (not illustrated) and in isolated cytoskeletons (Fig. 7 a and b). The *a* and *f* tubules of the R_3 root can be discerned in the loop region. The R_3CM appears as a dense band extending from the basal bodies to the cell posterior. The cytoplasmic microtubules nucleated from the R_1 root and the short flagellum basal body form the surface topology for the cell (Fig. 7 a and b) and converge in the cell posterior, perhaps with the R_3CM, to form the stalk (Fig. 7 c).

Immunostaining, using antibodies active against actin (monoclonal) and centrin (monoclonal, polyclonal), fails to demonstrate the presence of actin or centrin in the rhizoplast; a positive centrin reaction occurs on or very near the basal bodies and inconsistently in the loop region along the R_3 microtubules (not illustrated).

Feeding cup formation

Figure 8 is an illustration of a feeding cup reconstructed from a serially sectioned cell. Thin sections show a wider separation between the *a* and *f* tubules in the loop region of the R_3 root in cells with a cup forming (Fig. 9 a–c) than occurs in cells without feeding cups (Figs. 3 a and b and 4 a and b). The *f* tubule forms the rim of the feeding cup, and its circumference, determined from the reconstructed model, is approximately 3.2 μm. The *f* tubule has a striated coating (Fig. 9 a) that was not observed in cells lacking cups. The distal end of the *f* tubule is near the level of the basal bodies (not illustrated) while the distal end of the *a* tubule is approximately 4 μm beneath the basal bodies (Fig. 9 b–h). Because the *f* tubule terminates approximately 1 μm anterior to the *a* tubule in cells without a feeding cup (Fig. 5 h–j), an anteriorly directed sliding of the *f* tubule for approximately 3 μm (the increased circumference of the *f* tubule loop) accounts for the 4 μm distance between the distal ends of the *a* and *f* tubules in this cell. Furthermore, this cell was embedded on a glass slide and it was photographed before it was mounted for sectioning; the rim of the feeding cup measured 1 μm in diameter, or 3.14 μm in circumference. Therefore, the feeding cup rim forms as the *f* tubule slides anteriorly.

Such carefully controlled displacement of a microtubule is not limited to the *f* tubule, however. During feeding cup formation, the *a* tubule is seen displaced from the complex layered structure and towards the plasma membrane (Fig. 9 d–h; compare to Fig. 5 e–j). The *a* tubule has a striated coating, apparently resulting from associated strands of the rhizoplast that peeled away from the main body of the rhizoplast. No other microtubular movements associated with feeding cup formation were detected. A schematic diagram of the microtubular movements is illustrated in Fig. 10.

The surface area of the feeding cup increases as it forms, requiring additional membrane material. Two types of vesicles are present in the area of the forming cup, and one or both probably play a role in membrane growth. Type 1 vesicles are spheroid and empty in appearance (Fig. 11 c). Type 2 vesicles are elongate and sausagelike in shape and contain numerous beadlike inclusions (Fig. 11 d). Type 1 vesicles appear to fuse at the bottom of the feeding cup (Fig. 9 a–c) and provide depth to the developing feeding cup. Type 2 vesicles are often associated closely with the R_3 microtubules in the loop region (Fig. 11 d), but they also occur elsewhere in the cell.

Fig. 4. **a** and **b** Nonadjacent serial thin sections showing the position of the *a* and *f* tubules of the R_3 root and the R_4 microtubule. The R_3CM are indicated by the arrowhead, lying between the mitochondrion and rhizoplast. **b** 10° tilt. **c** The R_3 root (arrow) nucleates the R_3CM (arrowheads) that pass between the mitochondrion and rhizoplast; the chloroplast eyespot is closely associated. **d** Thick section showing the origin of the *a* and *f* tubules on the right side of the short flagellum and their distal ends passing the left side of the short flagellum and extending deep into the cell between the chloroplast and the complex layered structure (see text for details). The R_3CM are shown at the arrowhead. **e** and **f** Adjacent serial thin sections showing the striated appearance of the *a* and *f* tubules of the R_3 root. Bars: 500 nm

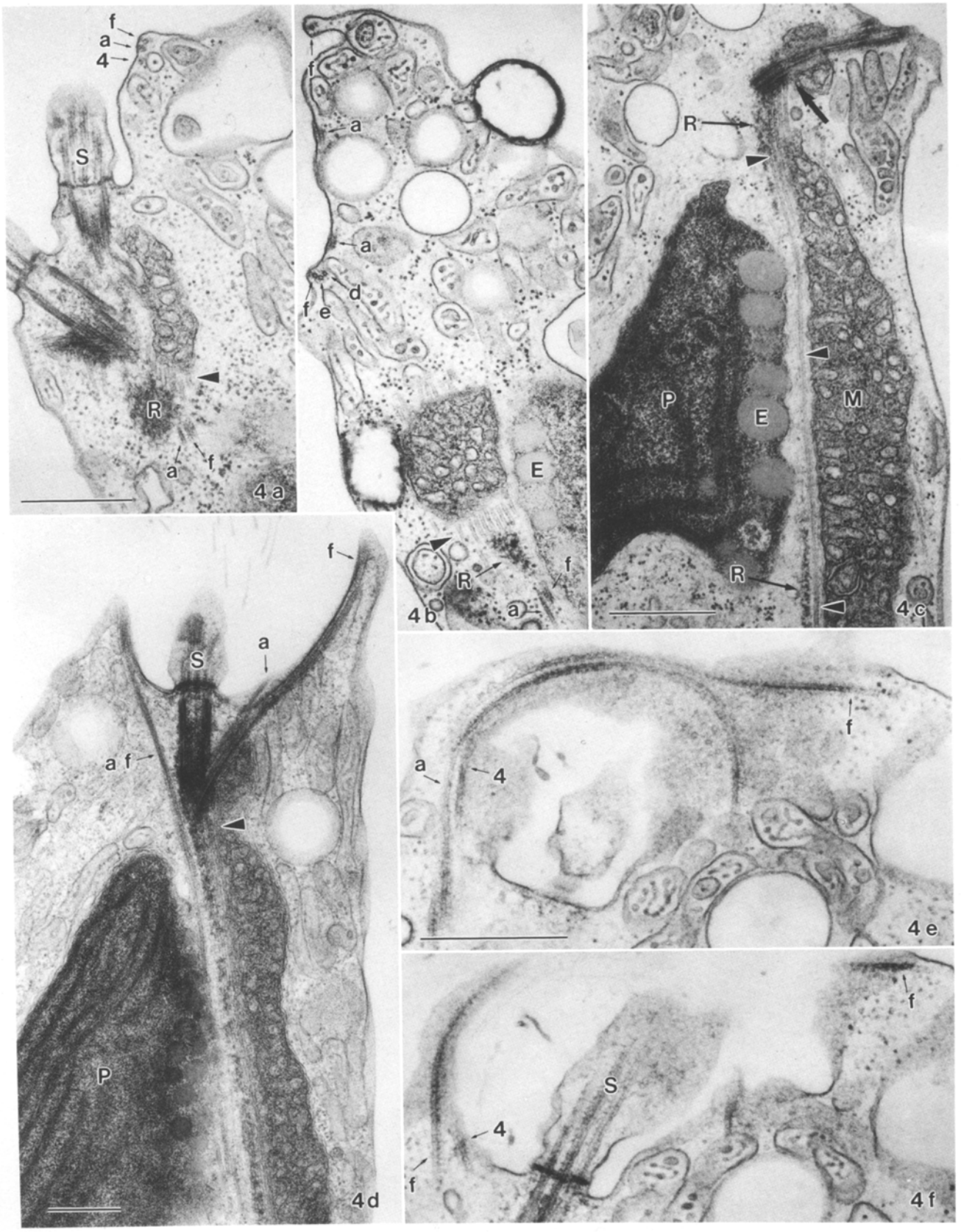
f
a
4
S
R
a
f
4a
f
a
a
d
f e
E
R
f
a
4b
R
P
E
M
R
4c
f
S
a
a f
P
4d
a
4
f
4e
S
4
f
f
4f

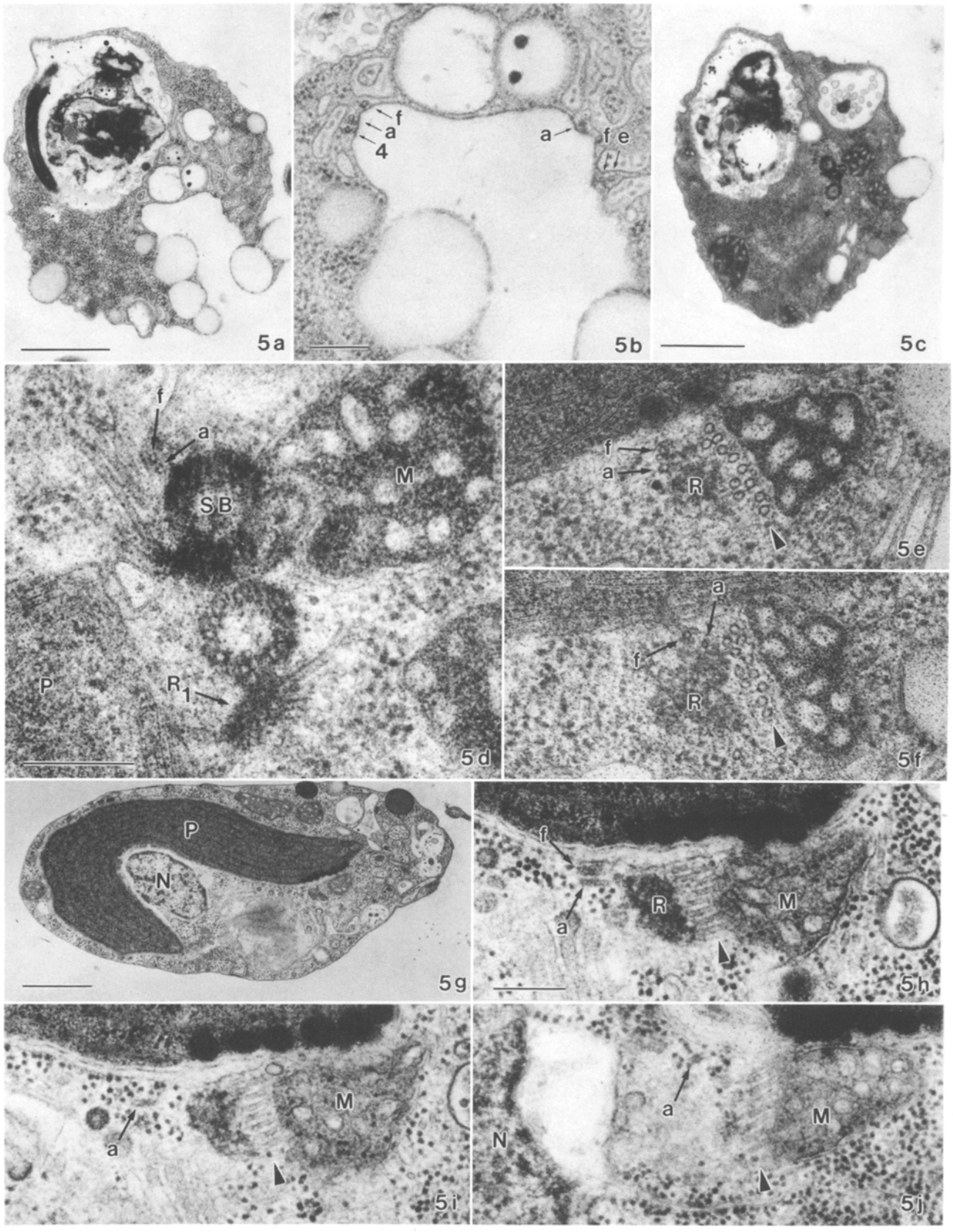
5a
5b
f
a
4
a
f e
5c
f
a
SB
M
P
R1
5d
f
a
R
5e
a
f
R
5f
P
N
5g
f
a
R
M
5h
a
M
5i
a
N
M
5j

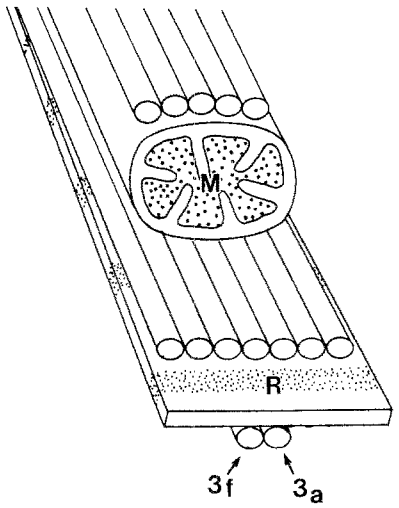

Fig. 6. A diagrammatic illustration of the complex layered structure. R_1 cytoplasmic microtubules are at the top, R_3 cytoplasmic microtubules (R_3CM) lie between the mitochondrion and the rhizoplast, and the *a* and *f* tubules of the R_3 root are at the bottom of the figure

Bacteria and other food particles are engulfed as the cup closes to form a food vacuole (Fig. 11 a and b). The food vacuole becomes larger than the food cup by the continued fusion of vesicles. Furthermore, cells do not always engulf an obvious food particle, forming food vacuoles with no bacterium or other prey (Fig. 11 a). The cause of these empty vacuoles may be a failure to engulf the food particle or a cellular decision to reject the food particle after the food cup forms.

Discussion

We do not know why an *Epipyxis* cell changes from the nonfeeding to the feeding stage. Feeding is widespread among the Chrysophyceae (Moestrup and Andersen 1991) and we assume feeding provides energy that supplements photosynthesis. For species such as *Ochromonas* or *Chrysosphaerella* where feeding does not require a complex morphogenesis, food uptake could be viewed as opportunistic. However, for *Epipyxis*, the relatively long and elaborate morphogenesis to the feeding state implies that feeding is not opportunistic but a predisposed "behaviour" that is under an elaborate cellular regulation.

The feeding apparatus in chrysophytes has constant as well as unique features. Many taxa appear to have an R_3 root that splits into two parts, the inner and outer loops: *Poterioochromonas* (Schnepf et al. 1977, Robinson and Quader 1980), *Chrysosphaerella* (Andersen 1990), *Dinobryon* (Owen et al. 1990 a), *Uroglenopsis* (Owen et al. 1990 b), *Epipyxis* (this paper), and *Ochromonas, Saccochrysis*, and others (unpubl. obs.). In all of these, the R_3 root consists of six microtubules at its proximal end. The *a* tubule forms at least part of the inner loop and the *f* tubule forms at least part of the outer loop. Also, the distal length of the *f* tubule passes under the basal bodies in all examined chrysophytes. However, the *f* tubule in *Chrysosphaerella* forms a coil of up to five gyres on top of the nucleus (Andersen 1990) while in *Epipyxis* it is long and straight. The distal path of the *f* tubule has not been determined for *Dinobryon* (Owen 1990 a), *Poterioochromonas* (Schnepf et al. 1977) and *Uroglenopsis* (Owen et al. 1990 b), but none of these appear to resemble either *Chrysosphaerella* or *Epipyxis*.

Because of the structural differences among the genera which have been studied (see Andersen 1991), it is difficult to formulate a unifying hypothesis for feeding cup formation among chrysophytes. *Ochromonas* and *Chrysosphaerella* (Andersen 1990) do not form an obvious feeding cup; instead, they form a "cave" or "pouch" where the two loops of the R_3 root separate. Because *Ochromonas* and *Chrysosphaerella* are not surrounded by a lorica, they can form a feeding "pouch" rather than the more obvious feeding "cup" found in *Epipyxis*. In an old drawing of *Dinobryon*, another loricate organism, Stein (1878) illustrates a "loop" that is almost certainly a feeding cup. Not all loricas are as confining as those of *Epipyxis* and *Dinobryon*. *Poterioochromonas* has a lorica that does not occlude the anterior region of the cell. Its feeding mechanism has not been described using electron microscopy, but feeding cups were illustrated when the genus was first de-

Fig. 5. a–f Selected serial thin sections showing the path of the *a* and *f* tubules. **a** Cell cross section through cell anterior showing food vacuole; the flagella are broken off below this level. **b** An enlarged view of **a** showing the position of the microtubules. **c** Cell cross section at the level of the basal bodies. **d** An enlarged view of **c** showing the *a* and *f* tubules passing near the short flagellum basal body. **e** and **f** Sections showing the *a* and *f* tubules lying near the rhizoplast; note the R_3CM (arrowhead) between the mitochondrion and rhizoplast. The *f* tubule is closely associated with the outer membrane of the chloroplast endoplasmic reticulum. **f** 10° tilt. **g** and **j** Selected serial thin sections showing the termination of the *f* and *a* tubules and the R_3CM (arrowheads). **g** Whole cell. **h** An enlarged view of **g** showing the last section containing an *f* tubule; note the close association between the *f* tubule and the outer membrane of the chloroplast endoplasmic reticulum. **i** Adjacent section showing only the *a* tubule. **j** Last section containing the *a* tubule; note the close proximity of the *a* tubule to the nucleus and the separation of the nuclear envelope, apparently due to a contraction of the rhizoplast. Bars: 1 μm in a, c, and g; 200 nm in b, d–f, i, and j

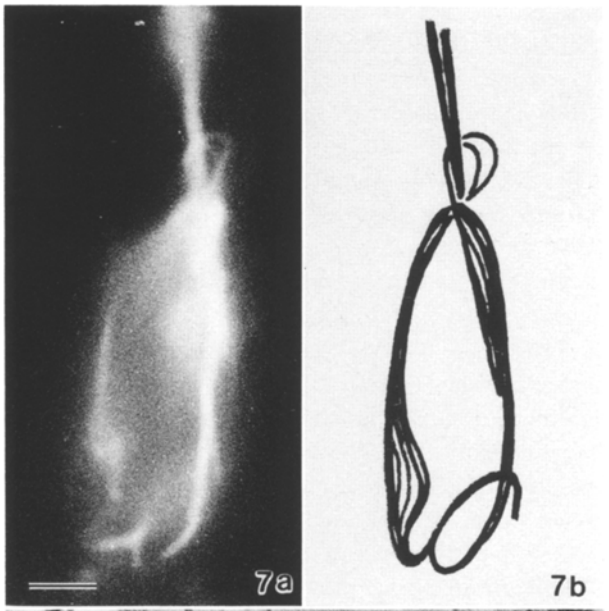

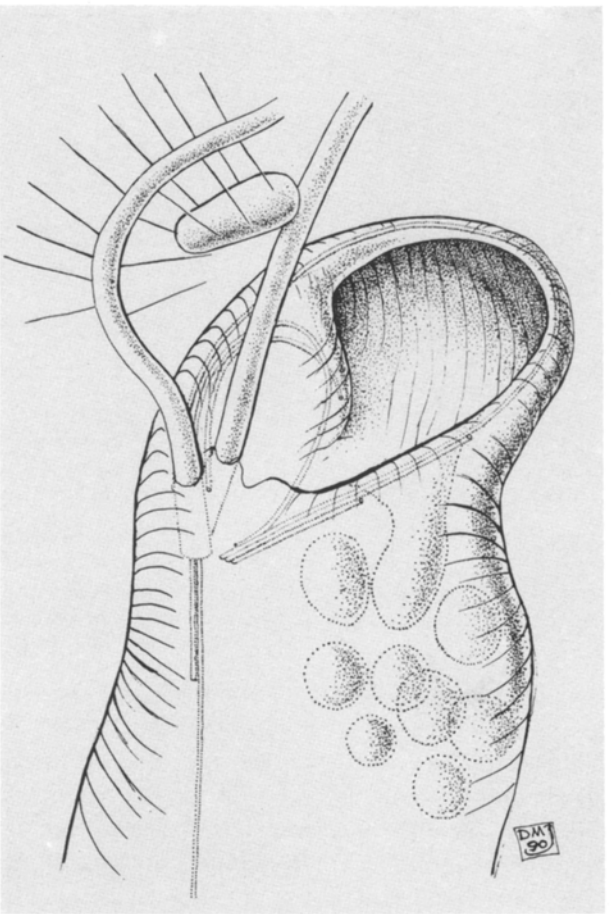

Fig. 8. A threedimensional illustration showing the *f* tubule widely separated from the *a* tubule forming a feeding cup. The illustration is from a model reconstructed from a serially sectioned cell (see Fig. 9)

scribed (Scherffel 1901) and they are similar to those of *Epipyxis*. Thus, a lorica may obstruct prey capture, and loricate cells may have adapted by forming a feeding cup that extends farther from the cell body.

Some of the mechanical features in feeding cup formation are simple and straight forward. We suggest that the *f* tubule, probably interacting with the *a* tubule and the R_4 root, slides up to form the enlarging rim of the cup. At the same time, vesicles fuse along the bottom and sides of the cup to increase its surface area and depth. How the cup closes, how the microtubules return to their pre-cup positions, and how the food vesicle changes size, shape and position after it is formed, is not yet determined.

Fig. 7. a An FITC labelled cell using an anti-tubulin antibody showing the separate *a* and *f* tubule loops at the cell anterior and the coalescence of cytoplasmic microtubules to form the stalk. **b** A diagrammatic interpretation of **a. c** Thick section showing the coalescence of microtubules to form the stalk. Bar: 1 μm in a and b; 500 nm in c

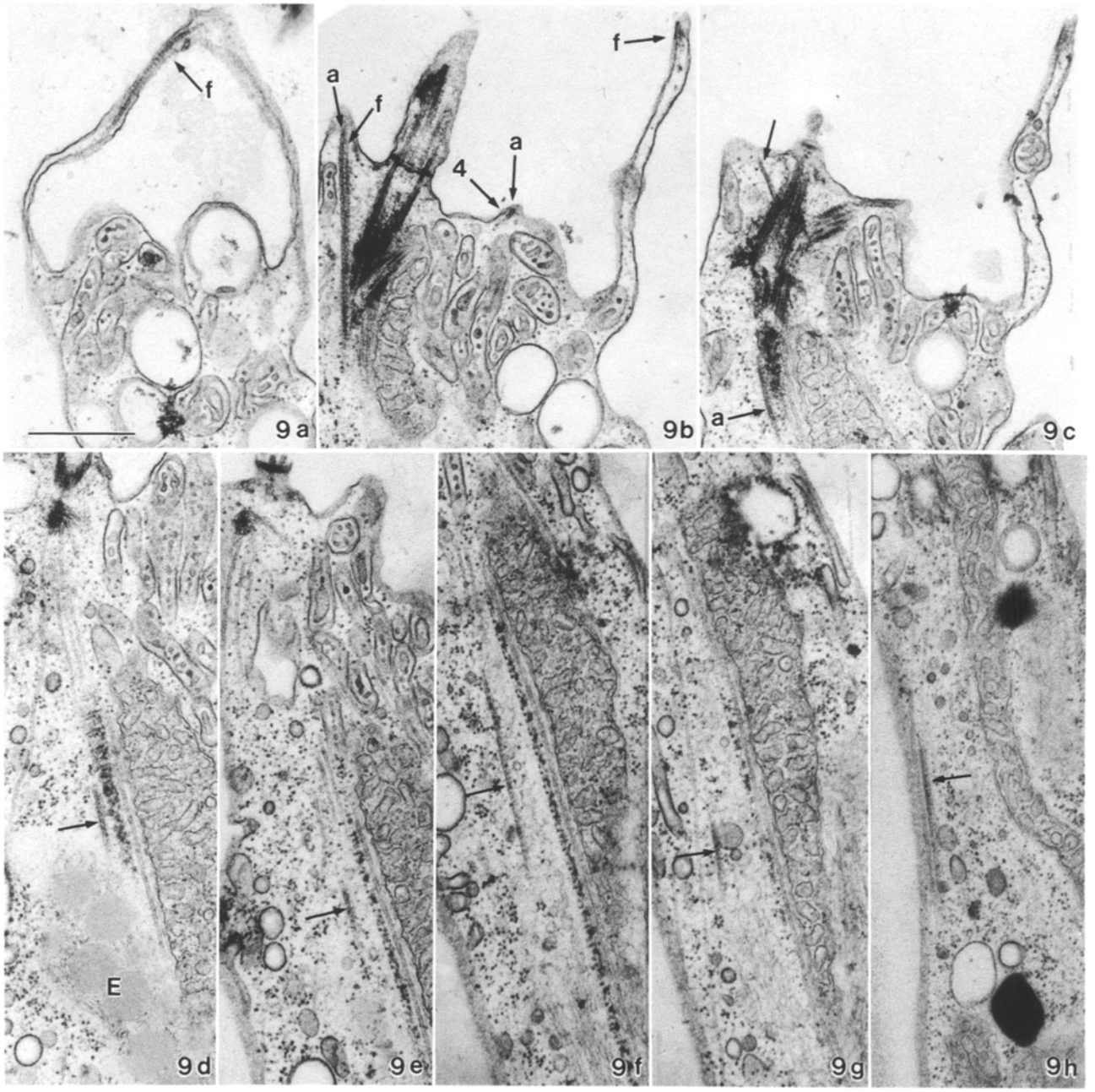

Fig. 9 a–h. Selected serial thin sections of a cell forming a feeding cup. **a** The *f* tubule along the left rim of the feeding cup. Section 1. **b** The *a* and *f* tubules passing the short flagellum basal body. Section 10. **c** The *a* tubule just after the *f* tubule discontinued. The proximal end of the R_4 root (arrow) is on upper surface of short flagellum basal body. Section 12. **d–h** The *a* tubule (arrow) as it becomes more widely spaced from the rhizoplast and finally lies along the cell surface. Note the heavy coating of rhizoplast-like material. Sections 17, 19–21, and 23, respectively. Bar: 500 nm

The closure of the cup to form a food vacuole after capture has proved too transient to document using electron microscopy. The short flagellum forms a sharp bend as the food particle is moved into the cup (Wetherbee and Andersen 1992). The R_4 root is attached directly on the short flagellum. The sudden bending of the flagellum may cause the R_4 root microtubule to disrupt its interaction with the *a* and *f* tubules of the R_3 root. If these microtubules are separated, a contractile element could close the cup, returning the microtubules to their original positions.

Striated fibers resembling those of the rhizoplast occur

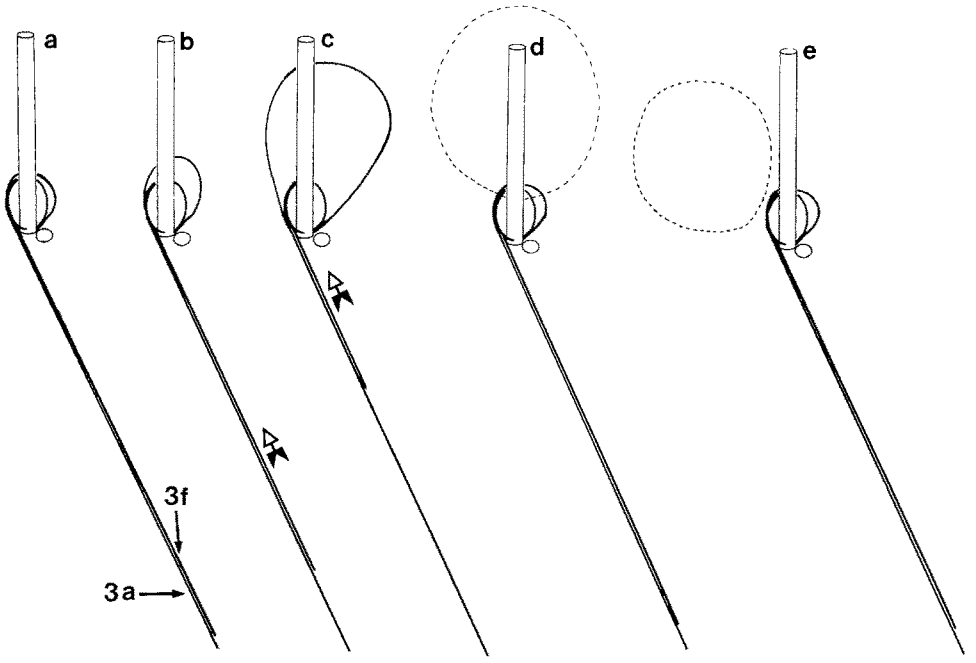

Fig. 10 a–e. A diagrammatic illustration showing the position of the *a* and *f* tubules before, during and after feeding cup formation. **a** The position of the *a* and *f* tubules before feeding cup formation. **b** and **c** The progressive anterior sliding of the *f* tubule to form the rim of the feeding cup. **d** and **e** The *f* tubule is returned to its original position and the feeding vacuole moves towards the left side of the cell and slightly posteriorly

on the *a* tubule during feeding cup formation (Fig. 8 e–h). Also, the *a* and *f* tubules are coated with a periodically striated material (Fig. 4 d–f). Rhizoplasts (= system II fibers) are known to contain centrin, a Ca^{++} sensitive contractile protein (Salisbury et al. 1984, Salisbury 1989). We have been unable to consistently demonstrate an immunological reaction on the feeding cup using anti-centrin antibodies. However, if present, centrin may play a role in closing the feeding cup.

Many questions still remain to be answered: What is the signal that initiates feeding cup formation? Is the mechanism of microtubular sliding driven by molecular motors? How is the feeding cup closed? The search for answers to these questions may lead to a better understanding of cellular regulation and function for other cells and systems. The complex yet distinctive features of the phagocytotic process in *Epipyxis* provide opportunities for dissecting cellular processes that are more obscure in other cells.

Acknowledgements

We wish to thank Dr. R. McIntosh and the staff of the High Voltage Electron Microscope Unit, Department of Molecular, Cellular and Developmental Biology, University of Colorado, Boulder, CO, U.S.A., for their assistance and use of facilities. Also, we thank Dr. David Assai for the monoclonal antitubulin antibody, and Dr. Jeffrey Salisbury for the monoclonal and polyclonal anti-centrin antibodies. Finally, we thank Dr. Dean Jacobson for preparing the illustration in Fig. 7. RAA acknowledges financial support from the National Science Foundation Grant no. BSR 8709222, and RW acknowledges financial support from the Australian Research Council. This is Bigelow Laboratory of Ocean Sciences contribution number 91023.

Fig. 11. a A cell with three food vacuoles. The middle vacuole contains particles but the other two vacuoles contain little or no obvious food particles; note the lorica scales on the right side. **b** A thick section showing a food vacuole containing a bacterium, the typical food item for this alga. Note the close association of the Type 2 vesicles near the lower left of the micrograph as well as several large Type 1 vesicles. **c** A thick section showing a row of Type 1 vesicles forming a chain below the area where the feeding cup forms. **d** A thick section showing the close association of the Type 2 vesicles with proximal end of the R_3 root, especially the *a* tubule. Two Type 1 vesicles lie between the *a* and *f* tubules. Bars: 500 nm

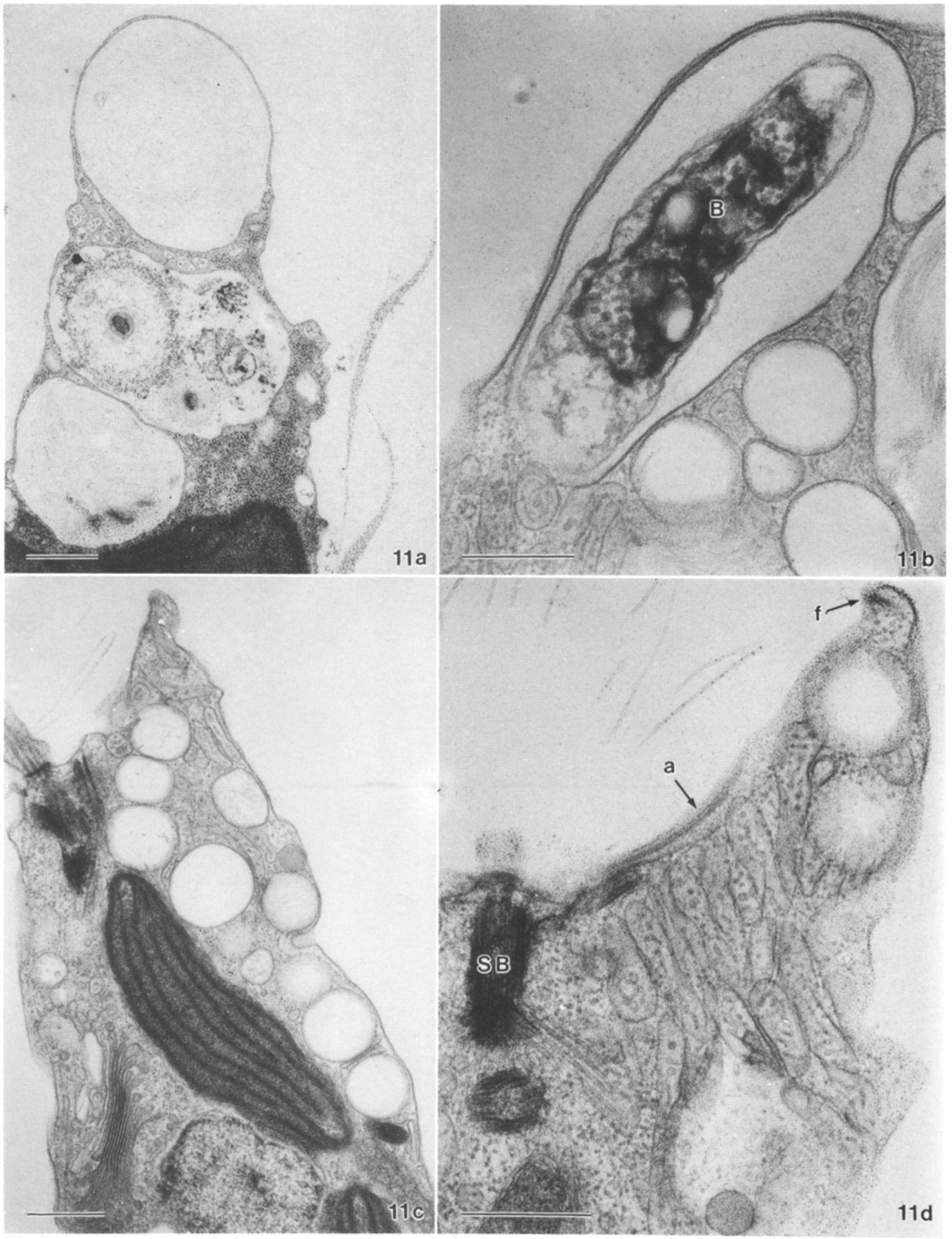
11a
B
11b
11c
f
a
SB
11d

References

Andersen RA (1990) Three-dimensional structure of the flagellar apparatus of *Chrysosphaerella brevispina* (Chrysophyceae) as viewed by high voltage electron microscopy stereo pairs. Phycologia 29: 86–97

– (1991) The cytoskeleton of chromophyte algae. Protoplasma 164: 143–159

Cienkowski L (1870) Über Palmellaceen und einige Flagellaten. Arch Mikrosk Anat Entwicklungsmech 6: 421–438

James-Clark H (1867) On the Spongiae Ciliatae as Infusoria Flagellata; or, observations on the structure, animality, and relationship of *Leucosolenia botryoides*. Bowerbank Mem Boston Soc Nat Hist 1: 305–340

Koutoulis A, McFadden GI, Wetherbee R (1988) Spine-scale reorientation in *Apedinella radians* (Pedinellales, Chrysophyceae): the microarchitecture and immunocytochemistry of the associated cytoskeleton. Protoplasma 147: 25–41

Lehman JT (1976) Ecological and nutritional studies on *Dinobryon* Ehrenb.: seasonal periodicity and the phosphate toxicity problem. Limnol Oceanogr 21: 646–658

Moestrup Ø, Andersen RA (1991) Organization of heterotrophic heterokonts. In: Patterson DJ, Larsen J (eds) The biology of free-living heterotrophic flagellates. Oxford University Press, Oxford (in press)

Owen HA, Mattox KR, Stewart KD (1990 a) Fine structure of the flagellar apparatus of *Dinobryon cylindricum* (Chrysophyceae). J Phycol 26: 131–141

– Stewart KD, Mattox KR (1990 b) Fine structure of the flagellar apparatus of *Uroglena americana* (Chrysophyceae). J Phycol 26: 142–149

Pascher A (1910) Chrysomonaden aus dem Hirschberger Grossteiche. I. Untersuchungen über die Flora des Hirschberger Grossteiches. Leipzig

Robinson DG, Quader H (1980) Topographical features of the membrane of *Poterioochromonas malhamensis* after colchicine and osmotic treatment. Planta 148: 84–88

Salisbury JL (1989) Alga centrin: calcium-sensitive contractile organelles. In: Coleman AW, Goff LJ, Stein-Taylor JR (eds) Algae as experimental systems. AR Liss, New York, pp 19–37

– Baron A, Surek B, Melkonian M (1984) Striated flagellar roots: isolation and partial characterization of a calcium-modulated contractile organelle. J Cell Biol 99: 962–970

Saville-Kent W (1880) A manual of Infusoria. 1. London

Sanders RW, Porter KG (1988) Phagotrophic phytoflagellates. In: Marshall KC (ed) Advances in microbial ecology. Plenum, New York, pp 167–192

Scherffel A (1901) Kleiner Beitrag zur Phylogenie einiger Gruppen niederer Organismen. Bot Z 59: 143–158

Schnepf E, Deichgräber G, Röderer G, Herth W (1977) The flagellar root apparatus, the microtubular system and associated organelles in the chrysophycean flagellate, *Poterioochromonas malhamensis* Peterfi (syn. *Posteriochromonas stipitata* Scherffel and *Ochromonas malhamensis* Pringsheim). Protoplasma 92: 87–107

Stein FR (1878) Der Organismus der Infusionsthiere, III. Abt., I. Hälfte. Leipzig

Stokes AC (1885) Notes on some apparently undescribed forms of fresh-water infusoria, no. 2. Am J Sci III 29: 313–328

Wetherbee R, Andersen RA (1992) Flagella of chrysophycean algae play an active role in prey capture and selection. Direct observations on *Epipyxis pulchra* using image enhanced video microscopy. Protoplasma 166: 1–7